

Shear-induced long-range alignment of BCC-ordered block copolymers

Prashant Mandare · H. Henning Winter

Received: 25 September 2006 / Accepted: 19 April 2007 / Published online: 12 June 2007
© Springer-Verlag 2007

Abstract Effect of large shear on an asymmetric block copolymer with nanospherical domains has been studied using rheology and small angle X-ray scattering. The material investigated was a triblock copolymer poly [styrene-*b*-(ethylene-*co*-butylene)-*b*-styrene] swollen in a midblock-selective solvent. When cooled below the order–disorder transition temperature (T_{ODT}), the system forms a locally ordered structure of grains with body-centered cubic (BCC) lattice. Isothermal shearing, either at constant rate or with large amplitude oscillatory shear (LAOS) at low frequencies and strain amplitude greater than or equal to 2.0, leads to the destruction of the BCC lattice (isothermal “shear melting”). Upon cessation of the shear, the BCC structure recovers with kinetics similar to the one after thermal quench from above T_{ODT} . Under certain experimental conditions, LAOS leads to alignment of the BCC lattice. The lattice orientation depends primarily on shearing frequency. At low frequencies, there exists an upper and lower bound on strain amplitude where monodomain textures can be obtained. Upon alignment, the modulus drops by about 30% of that of the polycrystalline structure. Measurement of rheological properties offers an indirect method for distinguishing between polycrystalline structure (grains) and monodomain texture.

Keywords Block copolymer · Large amplitude oscillatory shear · Flow induced orientation · BCC order · Monodomain

Introduction

Nanophase separation in block copolymers of uniform molar mass leads to formation of a periodic structure of nanoscale domains. The size, shape, and periodicity of these domains depend on the volume fraction of individual blocks, thermodynamic incompatibility, and thermo-mechanical history. Periodicity arises when these nanosize domains, after phase separation, further order into supramolecular structures of micron size. The morphology and ordering dynamics of the ordered phases has been the subject of extensive research for the past two decades. Several investigators have studied the nanophase separation and subsequent ordering in block copolymers upon cooling and its effect on the rheology for different morphologies. Time-resolved small angle X-ray scattering (SAXS) and small angle neutron scattering (SANS) were used to discern the evolution of the microstructure.

For binary block copolymers (two types of linear blocks) of highly asymmetric composition, the minor phase, upon phase separation, forms nanosize spheres in a continuous matrix of the major component. As the composition of the minor component is increased, first, cylindrical domains are observed, and then, for nearly symmetric composition, lamellae are formed upon phase separation.

A fundamental difference between spherical domain morphology and other morphologies of block copolymers (cylinders, lamellae) is its reduced molecular mobility. Whereas one-dimensional (lamellae) and two-dimensional (cylinders) structures allow molecules to rearrange in two or one direction, respectively, without leaving their respective domains, cubic structures have no such mobility. This is due to the fact that a deformation in any direction changes the intersphere distance causing a penalty in free energy. Because of this, cubic structures of block copoly-

P. Mandare · H. H. Winter (✉)
Department of Chemical Engineering,
University of Massachusetts,
Amherst, MA, USA
e-mail: winter@ecs.umass.edu

mers exhibit strikingly different rheological properties than other morphologies (Rosedale and Bates 1990; Kawasaki and Onuki 1990; Ryu et al. 1997; Kossuth et al. 1999).

In case of spherical domains, the nano-spheres arrange on a body-centered cubic (BCC) lattice, a process that is much slower than ordering of cylinders to form a hexagonal lattice or the ordering of lamellae (Sakamoto and Hashimoto 1998). This BCC lattice ordering is observed below a certain temperature known as the “lattice-ordering temperature (T_{LOT})” that is substantially lower than the nanophase separation temperature (also referred to as “order–disorder transition temperature,” T_{ODT} ; Kim et al. 1999; Schwab and Stühn 1996). However, recent work by Park et al. 2005 suggests that the former transition is not clearly defined. Such lattice ordering of the nanospheres without any flow leads to polycrystalline or grain structure with grain size of the order of a few microns (Sakamoto and Hashimoto 1998).

For one-dimensional (lamellae) and two-dimensional structures (cylinders), a great effort has been made to study the kinetics of ordering upon phase separation and flow-induced large-scale ordering (Almdal et al. 1992; Gupta et al. 1996; Winter et al. 1993). For cubic phases, a considerable amount of literature (McConnell et al. 1995; Almdal et al. 1993; Mortensen et al. 2002, Mortensen 2004, Hamley et al. 1998, Castelletto et al. 2005) exists on the flow-induced ordering. Soenen et al. 1997 found for a triblock copolymer that the rate of BCC-lattice ordering, when lowering the temperature below T_{LOT} , is highest at a temperature in between T_{LOT} and the glass transition temperature of the polystyrene (PS) phase. The sample was a poly[styrene-*b*-(ethylene-*co*-butylene)-*b*-styrene] (SEBS) swollen in a mid-block-selective hydrocarbon oil. Similar observations were noted for poly(styrene-*b*-ethylene-*alt*-propylene) in squalane (Liu et al. 2004).

For selectively swollen SEBS, Soenen et al. 1997 observed that the rate of structure formation is negligible above a certain strain amplitude indicating structure break-up because of flow. For PS–polyisoprene (PI) di- and triblocks, a zero shear viscosity was observed at very low shear rates (Sebastian et al. 2002a). In addition, for a variety of similar di- and triblock samples, the BCC lattice was reported to be present during flow at low deformation rates. However, the BCC order was destroyed by shearing at a constant rate when exceeding a certain critical stress (τ_c ; Sebastian et al. 2002b). This τ_c was found to be proportional to the low frequency plateau modulus of the cubic structure. The recovery of the broken structure after application of $\tau > \tau_c$ was found to be very similar to the ordering after a thermal quench from above T_{ODT} . To our knowledge, these were the first attempts to study “mechanical melting” of BCC-forming block copolymers.

The flow was found to have a strong effect on the BCC-ordered structure of a PS–polybutadiene (PB) diblock that

was swollen with a styrene-selective solvent dibutyl phthalate (Watanabe et al. 2001a). SANS profiles recorded immediately after shearing showed that the position of the primary peak remained unchanged, whereas the secondary and higher order peaks add to a broad tail up to a shear rate of 1.0 s^{-1} . This suggested that the BCC lattice is only mildly disrupted up to a shear rate of 1.0 s^{-1} . However, at the higher shear rate of 10 s^{-1} , the position of the primary peak shifted to low q values (increase in average spacing between the spherical domains) thereby indicating massive disruptions of the BCC lattice. Similar observations were noted for corresponding butadiene–styrene–butadiene triblock in dibutyl phthalate (Tan et al. 2003). This value of shear rate was found to be close to the concentration fluctuation frequency of PS–PB chains, which is obtained from the reciprocal of the terminal relaxation time as obtained from $G'-G''$ plots. Whereas the recovery of the diblock after shear was slowest at this shear rate, the recovery of the triblock after shear was observed to be independent of shear rate. It also was much slower than the recovery of a comparable diblock.

Almdal et al. 1993 used SANS in all the three directions to study the effect of large amplitude oscillatory shear (LAOS) on poly(ethylenepropylene) (PEP)–poly(ethylethylene) diblocks at elevated temperatures. LAOS at temperatures between 70 and 90 °C and with a strain amplitude of 1.0 and a shearing frequency of 0.02 rad/s generated a twinned BCC structure with $\{110\}$ planes oriented parallel to the shear planes. For the diblock of poly(styrene-ethylene-*alt*-propylene), in-situ SAXS studies during LAOS indicated different results (Okamoto et al. 1994). Under the experimental conditions (room temperature), the PS spheres were vitrified ($T_g \approx 62 \text{ °C}$) in the molten matrix of PEP ($T_g \approx -60 \text{ °C}$). With a shearing frequency of 0.0936 rad/s and strain amplitude of 0.5, in situ SAXS measurements indicated a preferential orientation of the BCC lattice with $\{110\}$ planes parallel to the shear plane. In addition, the total stress decayed during shearing as number of LAOS cycles increased. However, this preferential orientation of $\{110\}$ planes relaxed and stress recovered after the cessation of LAOS. SAXS studies also indicated that the BCC lattice was oriented only during LAOS but vitrified PS spheres remained undeformed. The strain amplitude imposed on the BCC lattice was nearly equal to the macroscopic strain amplitude (Okamoto et al. 1994).

LAOS led to an increase in degree of order and decrease in dynamic moduli of gels of $E_{40}B_{10}$ in aqueous K_2SO_4 (Pople et al. 1997). Upon cessation of LAOS, the moduli recovered to the original value (of less ordered structure). However, the large-scale structure was retained even after the cessation of shear. For diblocks of poly(oxyethylene)–poly(oxybutylene), LAOS was observed to induce macroscopic alignment of twinned BCC crystals (Hamley et al. 1998).

Shear-induced morphologies of the cubic-ordered triblock copolymer in a selective solvent have been studied under LAOS and by using in situ SANS (Mortensen et al. 2002). LAOS above certain strain amplitudes and within a certain frequency range leads to the alignment of grains producing single-domain textures. The minimum strain amplitude required to achieve this ordering was found to be the same as that where a crossover between the dynamic moduli is observed during strain-sweep experiments. The frequency window where this ordering was achieved is nearly the same where G' and G'' are nearly equal in the linear viscoelastic range. Depending on the strain amplitude and frequency, different orientations were generated. For the PS-PI diblock in decane, face-centered cubic crystals of the nanophase-separated diblock copolymer changed from a polycrystalline (powder pattern) to $\langle 111 \rangle$ sliding layers under the application of steady shear (McConnell et al. 1995). The transition occurred over a certain range of shear rates where the material exhibited hysteresis in steady shear stress vs shear rate data. For higher shear rates, $\langle 111 \rangle$ layers align within the shear plane. For BCC crystals, twinned structures were obtained under shear with $\langle 110 \rangle$ layers parallel to the shear plane. Higher shear rates caused shear melting with loss of the BCC lattice.

Rheology of the aligned structures has been studied for the PS-PB diblock swollen in tetradecane (Watanabe et al. 2001b). The plateau modulus was found to decrease by about 10% upon shear-induced ordering.

Despite several studies on shear-induced ordering of block copolymers, time scales of breaking/recovery of the structure and rheology of cubic phases of block copolymers that is ordered using flow are largely unexplored. The present study deals with the effect of a well-defined flow on a BCC-ordered structure in asymmetric block copolymers. The cubic structure in these block copolymers is highly sensitive to strain. The BCC lattice breaks in shear flow even at extremely low shear rates (Mandare and Winter 2006). In this paper, we study the recovery of the structure that was broken in shear and search for flow conditions that generate long-range ordered structure.

Materials and methods

The triblock copolymer of this study, SEBS of Shell (commercial name Kraton G1650), contains 29% PS, has a number average molecular weight $M_n=94,000$, and a polydispersity index of 1.15. For our experiments, the midblock of the polymer was selectively swollen with an extender oil (commercial name Fina Vestan) having a M_n of about 600. The details of the sample preparation are adopted from Soenen et al. 1997. All the samples used in this study contain 20% polymer (SEBS20). The T_{LOT} for

SEBS20 is about 120 °C, and the glass transition temperature of the PS domains is about 60 °C.

Experimental

Rheology and small angle X-ray scattering

A strain-controlled rheometer (ARES, TA instruments) was used for measuring rheological properties and for shear-induced ordering. Cone and plate fixtures with a cone angle of 0.1 rad and a diameter of 25 mm were used for all the experiments. The nominal gap for the cone was 0.0559 mm.

SAXS was used for the morphological characterization. SAXS was performed using Ni-filtered Cu $K\alpha$ radiation (0.154 nm wavelength) from a Rigaku rotating anode (operated at 40 kV, 200 mA). The X-ray beam was collimated by a set of three pinholes. The camera length calculated by silver behenate was approximately 1,195 mm. Scattering patterns were acquired with 10×15 cm² Fuji BAS-2500 ST-VA image plates and were read with a Fuji BAS-2500 image plate scanner. Samples from the rheometer were directly used in the SAXS setup. The incident beam was perpendicular to the shear planes as shown schematically in Fig. 1.

All experiments were carried out with a BCC-ordered sample. The sample preparation will be described next.

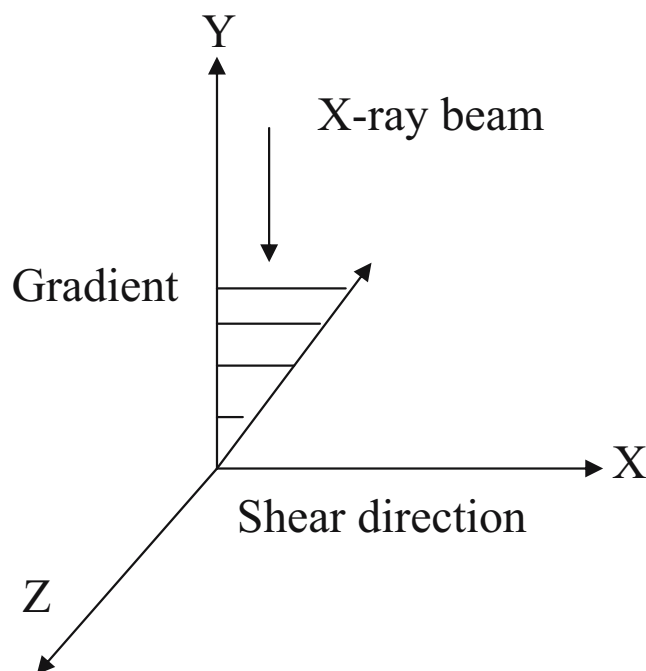


Fig. 1 Schematic of shear geometry and direction of incident beam for X-ray experiments

Preparation of BCC ordered sample

The sample was first heated to 150 °C into its single phase and kept at that temperature for 10 min to erase the thermo-mechanical history. Then, it was cooled to a temperature below T_{LOT} and kept there for BCC structure development. The isothermal ordering process was probed with a small amplitude oscillatory shear. The growth of the dynamic moduli after this thermal quench is shown in Fig. 2a. The evolution of $\tan\delta$ with time at different frequencies (Fig. 2b) shows that the sample exhibits a transition from liquid to solid. At the instant of transition (called “gel point”), the typical powerlaw relaxation behavior appears at low frequencies. Such powerlaw behavior is known for gelation because of network formation (Winter and Mours 1997), while here, gelation is due to repulsion between the molecular blocks and due to ordering.

The corresponding time required for the formation of critical gel is about 1,440 s, and the S and n values are about 2,868 Pa s^{*n*} and 0.646, respectively, where S and n are the stiffness and exponent in the Winter–Chambon gel equation describing the modulus of the critical gel $G(t) =$

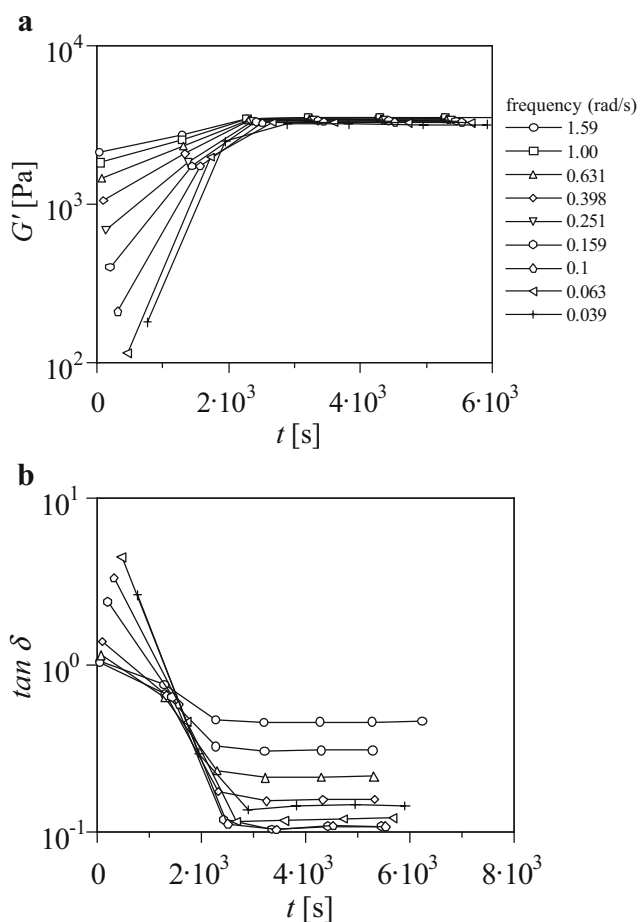


Fig. 2 Evolution of **a** storage modulus and **b** $\tan\delta$ during annealing at 100 °C after thermal quench from 150 °C

St^{-n} (Winter and Chambon 1986). The sample required about 3,000 s to reach steady values of moduli. As typical for physical gels, the storage modulus shows a frequency-independent plateau at low frequencies, while the loss modulus indicates that there is a finite longest relaxation time below which the sample can flow.

For most of the experiments described in this paper, the sample was annealed at 100 °C and then cooled to room temperature. This resulted in a nanophase-separated BCC-ordered structure. Concentric SAXS rings from such samples (Fig. 3) indicate the polycrystalline order. The BCC lattice spacing as determined from the position of the primary peak is about 28 nm. This ordered SEBS20 sample served as the initial condition for shear experiments throughout this paper.

Mechanical “melting”

The fragility of the formed structure was probed by applying two different types of large strain. The annealed sample was subjected to either LAOS or to shearing at a constant shear rate for a specified time. In initial experiments, immediately after the flow was stopped, the sample was quenched to room temperature, and SAXS was performed. In subsequent experiments, the broken structure was allowed to heal after the flow was stopped. For that purpose, the sample was kept at high temperature, and recovery of the sample was followed by time-resolved mechanical spectroscopy as explained by Mours and Winter (1994). Then, the sample was quenched to room temperature for SAXS characterization.

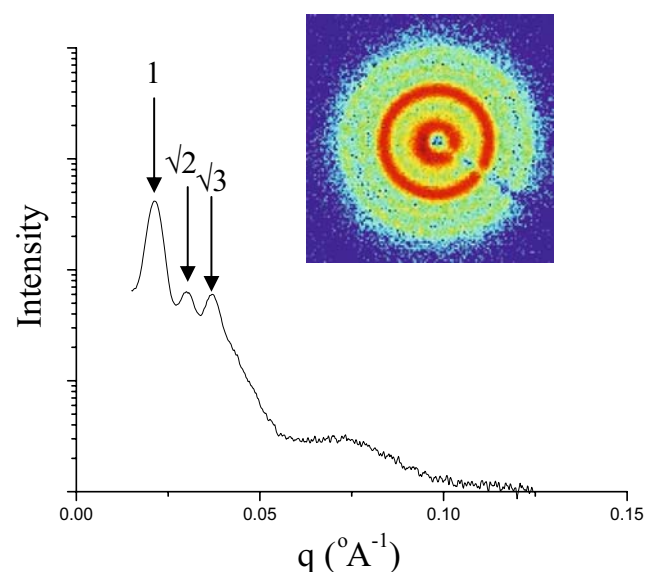


Fig. 3 SAXS profile of SEBS20 annealed at 100 °C and recorded at room temperature

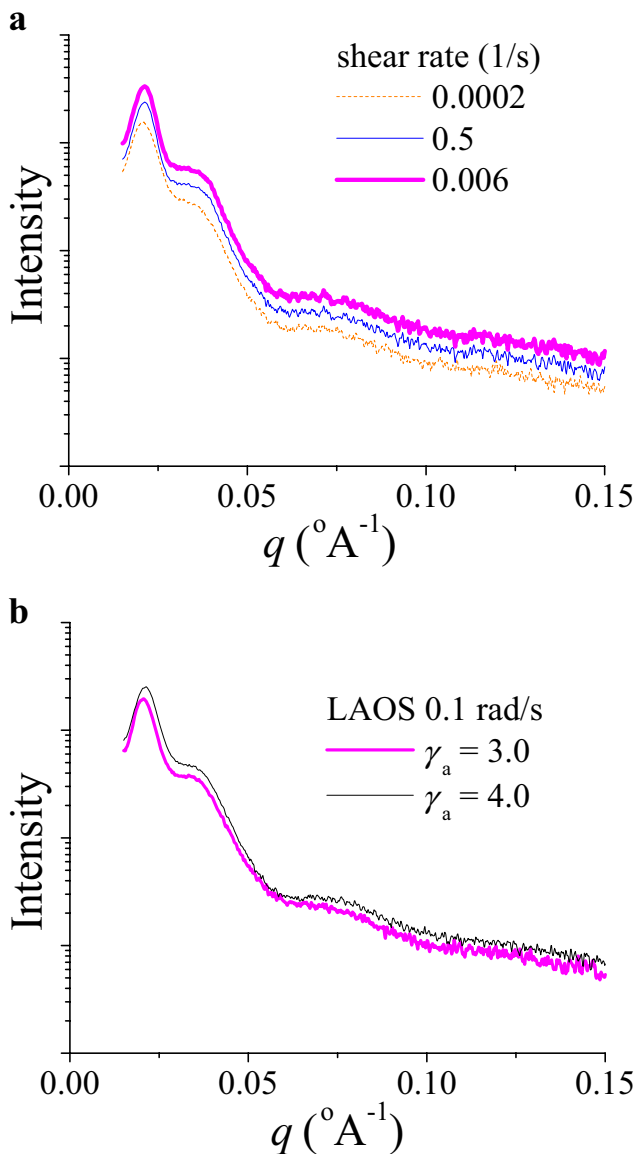
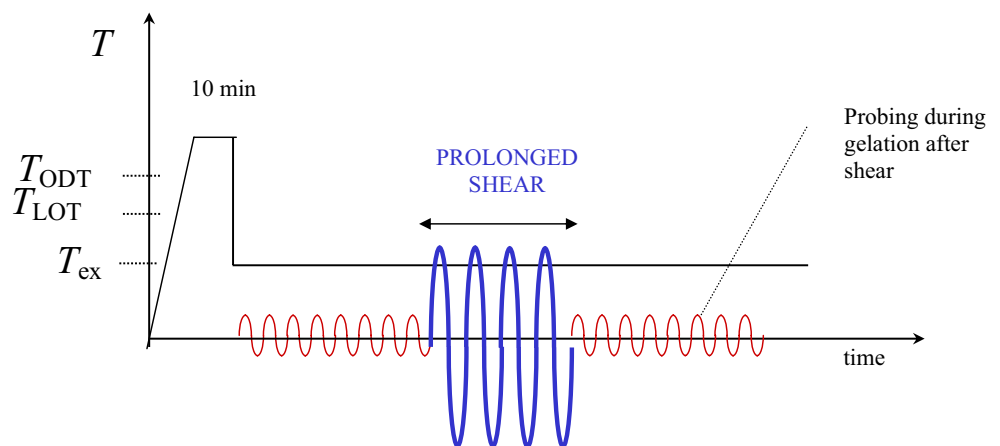


Fig. 4 **a** SAXS profile recorded on SEBS20 after sudden quench after shear at constant rate. A broad shoulder after the primary peak indicates liquid-like short-range order. **b** SAXS profile recorded on SEBS20 after sudden quench after LAOS at $\omega=0.1$ rad/s. A broad shoulder after the primary peak indicates liquid-like short range order

Fig. 5 Schematic of temperature and shear protocol used to study the recovery of sample after LAOS



Results

Effect of shear on formed structure

A quiescently ordered SEBS20 sample (Figs. 2, 3) was subjected to large shear strain (both constant shear and oscillatory). For the startup of shear, the shear rate was varied from 2×10^{-5} to 2.0 s^{-1} . For LAOS, both the shearing frequency and strain amplitude were varied. Leveling off of the stress response during shearing indicated that the “rheological” steady state had been reached and the breaking of the structure had reached a balance with some sort of dynamic assembly process.

The temperature during shearing was kept constant at $100 \text{ }^\circ\text{C}$ for all experiments. After reaching steady-stress levels, shearing was stopped, the sample was quenched to room temperature, and SAXS was performed. For LAOS, the shearing frequency was kept constant at 0.1 rad/s . Three different strain amplitudes were used, $\gamma_a=2.0, 3.0,$ and 4.0 . Figure 4a shows the SAXS profiles recorded after shearing at different shear rates, and Fig. 4b shows the SAXS profile recorded after LAOS. The BCC lattice was destroyed by shearing at a constant rate and by LAOS under all experimental conditions when the strain amplitude was greater than 2.0. SAXS results immediately after cessation of LAOS at low frequencies with $\gamma_a \leq 1.0$ are discussed in the next section.

Recovery after cessation of large shear

A major question for this research was how the structure that is broken because of shear can heal and how the order can establish itself. To study this, the starting point was again a quiescently ordered SEBS20 sample at $100 \text{ }^\circ\text{C}$ (Figs. 2, 3).

Large shear (oscillatory or constant rate) was applied to this sample at $100 \text{ }^\circ\text{C}$. When such a sample was quenched to room temperature, the SAXS studies always indicated that the BCC order was lost under all shearing conditions

(Fig. 4a,b). To study how such a broken sample can heal itself, annealing was carried out on the sample immediately after cessation of a large shear. Figure 5 shows a schematic diagram of temperature and shear protocol. The course of the recovery was followed by dynamic mechanical spectroscopy (see dynamic moduli of Fig. 6). When the dynamic moduli reached steady values, the probing was stopped, the sample was quenched to room temperature, and SAXS was performed to determine the presence/absence of the BCC lattice.

Figure 6 shows the recovery kinetics of the sample that was sheared at 100 °C using LAOS at $\omega=0.1$ rad/s. Results for four different strain amplitudes ($\gamma_a=1.0, 2.0, 3.0,$ and 4.0) are shown in Fig. 6a-d, respectively. The recovery kinetics and the final values of the moduli are dependant on the strain amplitude during LAOS. In particular, when the strain amplitude was greater than or equal to 2.0, samples recovered with the same time scales and to the same final moduli values as when it was quenched from a temperature above T_{ODT} and annealed (ref Figs. 2, 3). However, when the strain amplitude was less than 2.0, the final steady values of the modulus was reduced by about 30% compared to the sample that was quiescently ordered after thermal

Fig. 7 SAXS profile on a recovered sample after LAOS with $\omega=0.1$ rad/s; $T=100$ °C; **a** $\gamma_a>2.0$; **b** $\gamma_a=1.0$

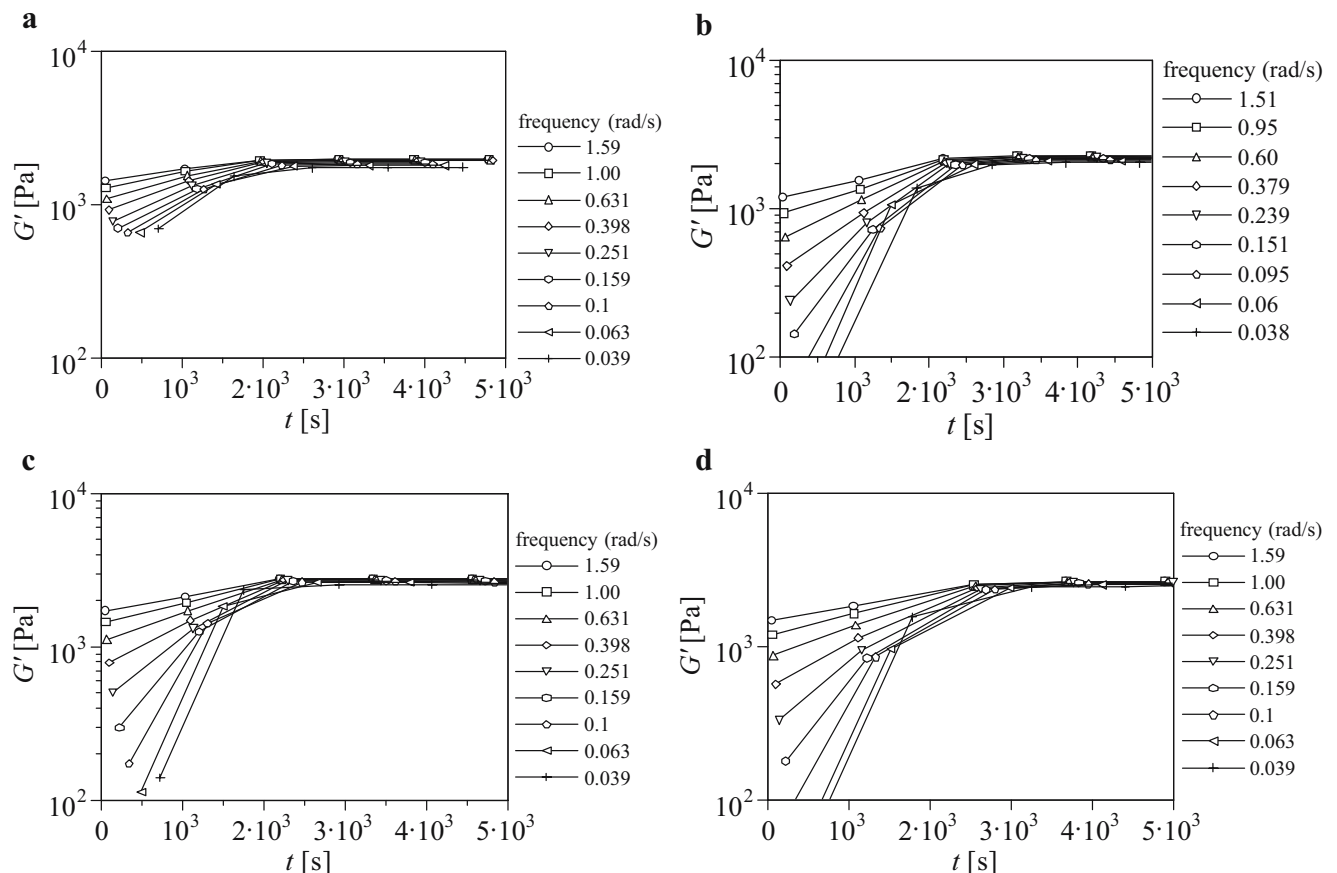
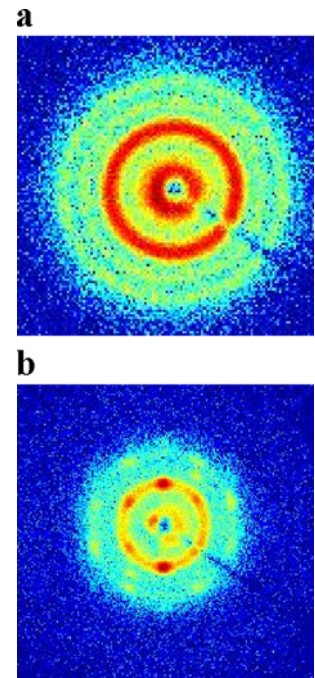


Fig. 6 Growth of storage moduli after LAOS with $\omega=0.1$ rad/s and at different strain levels; $T=100$ °C; **a** $\gamma_a=100\%$; **b** $\gamma_a=200\%$; **c** $\gamma_a=300\%$; **d** $\gamma_a=400\%$

quench from T_{ODT} . Moreover, the recovery was faster after the LAOS with $\gamma_a \sim 1.0$ with the initial moduli being relatively large compared to the samples that had been broken by larger strains.

The SAXS experiments on the “recovered” samples showed that under all conditions, the sample recovered with a BCC lattice. For $\gamma_a > 2.0$, the isotropic rings in the SAXS pattern indicate that the sample was polycrystalline (Fig. 7a) similar to that after thermal quench. Whereas, when $\gamma_a < 2.0$, the sample recovered with highly oriented structures. This is reflected in a near-symmetric sixfold pattern in the SAXS experiments (Fig. 7b). This structure has a modulus 30% less than the polycrystalline structure. Thus, measurement of rheological properties during recovery after LAOS offers an indirect tool (see Fig. 6) to distinguish between polycrystalline and aligned structures. A few SAXS experiments were performed immediately after shearing the sample with a frequency of 0.1 rad/s and a strain amplitude of 1.0 (not allowing the sample to recover). The scattering profiles on these samples also showed a near-symmetric sixfold pattern similar to Fig. 7b indicating that the highly ordered structures are formed sometime during the shearing. Annealing does not lead to any major changes to the scattering pattern; only the observed moduli at low frequencies increase slightly during annealing, indicating that shear melting does not occur when the strain amplitude is less than 1.0.

Shearing the sample using a constant shear rate leads to somewhat different results. The dynamic moduli after recovery were the same as those for quiescent ordering for all the shear rates used in the study. However, the time scales for the recovery were different. At low shear rates, the recovery was fast, whereas at higher rates, the recovery was slow and similar to the one after thermal quench. The SAXS results after recovery showed only the polycrystalline state.

Shear-induced large-scale ordering

During recovery after LAOS, it was realized that when the strain amplitude was less than 2.0, the samples recovered with highly oriented structures (Fig. 7b). In the following, a systematic investigation of this phenomenon is carried out to map a frequency/strain region where large-scale ordering is observed. Such a study has been performed earlier for SEBS20 (Mortensen et al. 2002). However, only the higher end of the frequency window (where G' and G'' are parallel and almost equal) was explored, and rheological observations were not reported. The purpose of this work was to extend this frequency window to lower frequencies and to observe the effect of large-scale ordering on the rheology of the material.

In initial experiments, a constant frequency was chosen at a value that falls in a region where a plateau is observed

in G' (0.5–0.001 rad/s at 100 °C). An annealed sample was sheared at this constant frequency for a period of 1 h. Higher shearing times were used at the lower frequency (up to 24 h for 0.001 rad/s) to allow a considerable number of shearing cycles. After shearing, the sample was annealed isothermally and then quenched for SAXS characterization. In all the SAXS experiments, the beam was parallel to the shear gradient.

It was observed that up to a shearing frequency of 0.01 rad/s, shearing with a strain amplitude of 1.0 leads to formation of a nearly symmetric sixfold pattern. Such an orientation has been observed earlier for SEBS (Mortensen et al. 2002) and for poly(ethylenepropylene)–poly(ethylene) (Almdal et al. 1993). This corresponds to the orientation where the $\{111\}$ plane is parallel to the shear plane. At a frequency of 0.001 rad/s, even after 24 h of shearing, highly oriented structures were not observed in SAXS.

At a frequency of 0.1 rad/s, the strain amplitude was varied between 0.25 and 4.0. The shearing time was kept constant at 1 h for each strain amplitude. It was observed that a minimum strain amplitude of 0.5 was required for the sixfold pattern to develop. Below this amplitude, the sample developed a structure with a polycrystalline pattern similar to Fig. 3. In addition, a strain amplitude of greater than or equal to 2.0 caused shear melting, and the sample recovered with a polycrystalline pattern upon annealing.

For comparison, a different frequency region was chosen (1.0–60 rad/s). A frequency of 1.0 rad/s coincides the transition from the plateau region of G' to the growth region with an increase in frequency. In this frequency window, a fourfold pattern was observed with a higher strain amplitude of 1.0 (Fig. 8a). At a lower strain amplitude (0.5), a different orientation is observed upon shearing that corre-

Fig. 8 SAXS profile on a recovered sample after LAOS with $\omega = 6.3$ rad/s; $T = 100$ °C; **a** $\gamma_a = 1.0$; **b** $\gamma_a = 0.5$

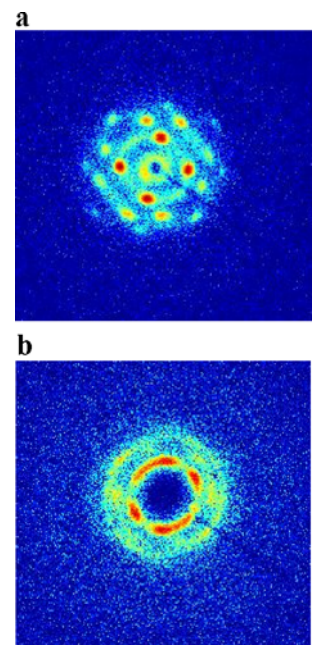


Table 1 frequency and strain during LAOS and the type of structure obtained after shearing

Frequency (rad/s)	Strain (%)	Type of structure			
		{110}/<111> (Fig. 8a)	{100}/<011> (Fig. 8b)	{111}/<112> (Fig. 7b)	Polycrystalline (Fig. 7a)
20	100	X			
10	100	X			
10	50		X		
6.3	100	X			
6.3	50		X		
1.0	100	X			
0.5	100			X	
0.1	>200				X
0.1	100			X	
0.1	50			X	
0.1	25				X
0.01	100			X	
0.001	100				X

sponds to an anisotropic scattering pattern (Fig. 8b). The pattern in Fig. 8b has two sharp meridional reflections and two sharp equatorial reflections. The fourfold pattern has been observed earlier for PS–PI under steady shear (McConnell et al. 1995) and for SEBS20 (Mortensen et al. 2002). The anisotropic pattern (Fig. 8b) has been reported only by Mortensen et al. 2002. The fourfold pattern corresponds to the orientation where the {110} plane/<111> direction is parallel to the shear plane/direction (twinned BCC structure). The asymmetric pattern is basically a two-dimensional powder with the {100} plane/<011> direction parallel to the shear plane as discussed in detail by Mortensen et al. 2002. In this case, only a part of the sample is oriented, whereas the remaining part is in powder

form. Table 1 reports the frequency and strain amplitude used and also the final orientation as observed by SAXS.

Shin et al. 2000 measured the deformations imposed on the lattice (change in domain spacing) and on nanospheres during LAOS. The sample consisted of soft spheres of poly (ethylene-*alt*-propylene) in hard matrix of PS. The temperature used was well above the T_g of nanospheres and slightly above the T_g of PS. The results showed that at 95 °C and with $\omega=0.0944$ rad/s, $\gamma_a=0.41$, the imposed strain on lattice is about 70% of the macroscopic strain and that on the spheres is about 40% of the macroscopic strain. It is emphasized that the frequency of 0.0944 rad/s corresponds the region where G' and G'' are parallel to each other (high-frequency region in this study). Spheres in the study of Shin

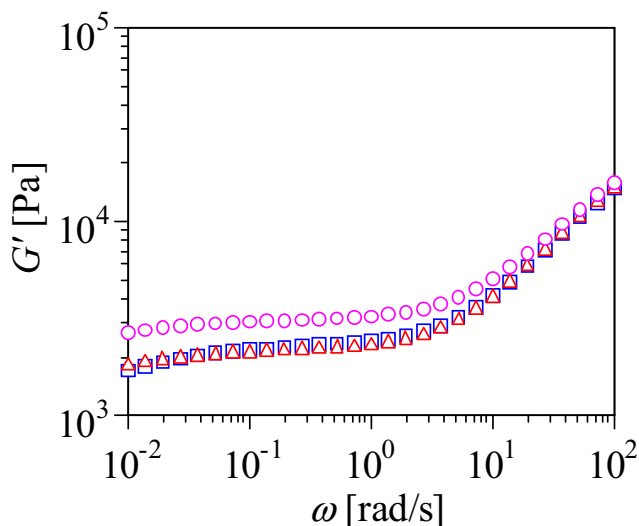


Fig. 9 Comparison of the frequency sweeps at 100 °C. *Triangles*: Sample ordered at $T=100$ °C using $\omega=6.3$ rad/s and $\gamma_a=100\%$ (Fig. 8a). *Squares*: Sample ordered at $T=100$ °C using $\omega=0.1$ rad/s and $\gamma_a=100\%$ (Fig. 7b). *Circles*: Sample annealed at 100 °C after thermal quench (Figs. 2, 3)

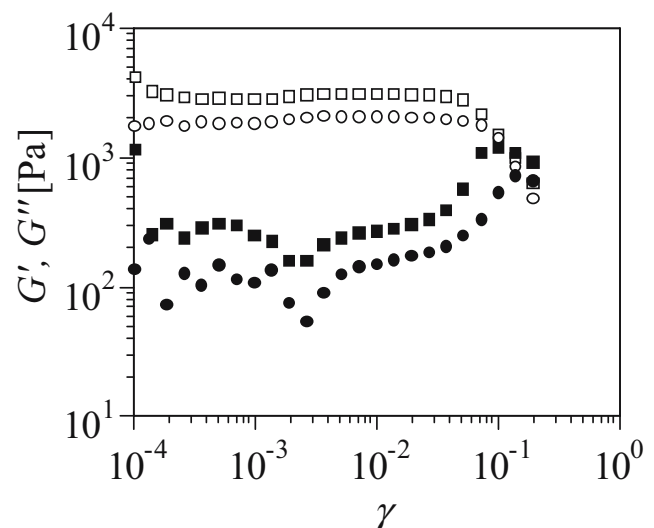


Fig. 10 Comparison of strain sweep at 0.1 rad/s, $T=100$ °C. *Squares*: Sample annealed at 100 °C after thermal quench (Figs. 2, 3). *Circles*: Sample ordered at $T=100$ °C using $\omega=0.1$ rad/s and $\gamma_a=100\%$ (Fig. 7b)

et al. 2000 are softer and hence easier to deform than the PS spheres in this study. On the other hand, the material in this study has a matrix that is softer and easier to deform than the PS matrix of Shin et al. 2000. This leads us to hypothesize that under our experimental conditions of high frequency (>1.0 rad/s), most of the deformation during LAOS is imposed on the BCC lattice that leads to a change in the interdomain spacing, whereas the PS spheres essentially maintain their shape. There is an energy penalty associated with this change in the PS domain spacing that can be minimized when a direction in the BCC lattice containing the highest density of PS spheres is aligned parallel to the shear direction. For the BCC lattice, this direction is $\langle 111 \rangle$, and the plane that has the highest density of PS spheres is the $\{110\}$ plane. This explains the observed twinned structure at high frequencies with the $\{110\}$ planes parallel to the shear plane. The origin of other two structures (Figs. 7b and 8b) is still unclear.

Dynamics of polycrystalline structure vs dynamics of aligned structure

Rheology of the highly oriented structure was studied using small amplitude oscillatory shear, and its strain sensitivity was probed in strain-sweep experiments. These results are compared with those for the polycrystalline structure (Fig. 9). The oriented structures, with different orientations, exhibit a plateau in G' at low frequencies similar to the one for the polycrystalline structure. However, the magnitude of this plateau is about 30% lower than that for the polycrystalline structure. In addition, the oriented structure exhibits a minimum in G'' at relatively lower frequencies than that for the polycrystalline. This indicates that even this highly ordered structure behaves as soft solids and that it will eventually flow at very low frequencies. It is interesting to see that all the highly oriented structures, with different orientations, exhibit the same rheological behavior with the plateau modulus being 30% less than that of the annealed sample.

A comparison of strain-sweep data on the oriented and polycrystalline structure (Fig. 10) indicates that the strain sensitivity of the material upon alignment is nearly the same as that for the quiescently ordered material.

Conclusions

SEBS20 under nanophase-separated conditions forms a BCC lattice with spheres of PS embedded in the matrix of EB. This three-dimensional order is destroyed under nonlinear deformations (constant rate as well as LAOS) giving rise to a liquid-like short-range ordering of PS spheres in the midblock. Upon cessation of the shear, the

broken structure heals, with ordering kinetics and morphology that depend on the shearing conditions. Shearing under constant rate as well as LAOS with $\gamma_a \geq 2.0$ leads to “mechanical melting.” The structure broken under these conditions recovers with kinetics similar to the one after thermal quench from above T_{ODT} . In addition, the morphology of the recovered structure is similar to the one after thermal quench (polycrystalline).

Highly oriented structures are achieved only by LAOS with $\gamma_a \leq 1.0$ but not by shearing at constant rate. The orientation achieved by such LAOS is dictated by the shearing frequency. At low frequencies (G' plateau), $\{111\}$ planes are oriented parallel to the shear plane. At low frequencies, there exists an upper and lower bound of strain amplitude between which this oriented structure can be obtained. At higher frequencies (G' and G'' parallel), $\{110\}$ planes are aligned parallel to the shear planes. All the different oriented structures exhibit a similar rheological pattern with a plateau modulus that is 30% less than that of the polycrystalline structure.

Acknowledgment This project is supported by the National Science Foundation (DMR-0213695) through the Materials Research Science and Engineering Center (MRSEC) at the University of Massachusetts Amherst.

References

- Almdal K, Koppi KA, Bates FS, Mortensen K (1992) Multiple ordered phases in a block copolymer melt. *Macromolecules* 25:1743–1751
- Almdal K, Koppi KA, Bates FS (1993) Dynamically sheared body-centered-cubic ordered diblock copolymer melt. *Macromolecules* 26:4058–4060
- Castelletto V, Hamley IW, Yuan X-F, Kelarakis A, Booth C (2005) Structure and rheology of aqueous micellar solutions and gels formed from an associative poly(oxybutylene)-poly(oxyethylene)-poly(oxybutylene) triblock copolymer. *Soft Matter* 1:138–145
- Gupta VK, Krishnamoorti R, Chen ZR, Kornfield ZA, Smith SD, Satkowski MM, Grothaus JT (1996) Dynamics of shear alignment in a lamellar diblock copolymer: interplay of frequency, strain amplitude and temperature. *Macromolecules* 29: 875–884
- Hamley IW, Pople JA, Fairclough JPA, Ryan AJ, Booth C, Yang YW (1998) Shear induced oriental transitions in the body centered cubic phase of a diblock copolymer gel. *Macromolecules* 31:3906–3911
- Kawasaki K, Onuki A (1990) Dynamics and rheology of diblock copolymers quenched into nanophase separated states. *Phys Rev, A* 42:3664–3666
- Kim JK, Lee HH, Sakurai S, Aida S, Masamoto J, Nomura S, Kitagawa Y, Suda Y (1999) Lattice disordering and domain dissolution transitions in polystyrene-block-poly(ethylene-co-but-1-ene)-block-polystyrene triblock copolymer having a highly asymmetric composition. *Macromolecules* 32:6707–6717
- Kossuth MB, Morse DC, Bates FS (1999) Viscoelastic behavior of cubic phases in block copolymer melts. *J Rheol* 43:167–196

- Liu Z, Shaw MT, Hsiao BS (2004) Ordering kinetics of BCC morphology in diblock copolymer solutions over a wide temperature range. *Macromolecules* 37:9880–9888
- Mandare P, Winter HH (2006) Ultra-slow dynamics in asymmetric block copolymers with nano-spherical domains. *Colloid Polym Sci* 284:1203–1210
- McConnell GA, Lin MY, Gast AP (1995) Long range order in polymeric micelles under steady shear. *Macromolecules* 28:6754–6764
- Mortensen K (2004) Three-dimensional crystallographic determination of the body-centered-cubic morphologies of shear-aligned block copolymer systems. *J Polym Sci B* 42:3095–3101
- Mortensen K, Theunissen E, Kleppinger R, Almdal K, Reynaers H (2002) Shear induced morphologies of cubic ordered block copolymer micellar networks studied by in situ small angle neutron scattering and rheology. *Macromolecules* 35:7773–7781
- Mours M, Winter HH (1994) Time resolved rheometry. *Rheol Acta* 33:385–397
- Okamoto S, Saijo K, Hashimoto T (1994) Dynamic SAXS studies of sphere-forming block copolymers under large oscillatory shear deformation. *Macromolecules* 27:3753–3758
- Park MJ, Char K, Bang J, Lodge TP (2005) The order–disorder transition and critical micelle temperature in concentrated block copolymer solutions. *Macromolecules* 38:2449–2459
- Pople JA, Hamley IW, Fairclough JPA, Ryan AJ, Komanschek BU, Gleeson AJ, Yu GE, Booth C (1997) Ordered phases in aqueous solutions of diblock oxyethylene/oxybutylene copolymers investigated by simultaneous small angle X-ray scattering and rheology. *Macromolecules* 30:5721–5728
- Rosedale JH, Bates FS (1990) Rheology of ordered and disordered symmetric poly(ethylenepropylene)–poly(ethylethylene) diblock copolymers. *Macromolecules* 23:2329–2338
- Ryu CY, Lee MS, Hajduk DA, Lodge TP (1997) Structure and viscoelasticity of matched asymmetric diblock and triblock copolymers in the cylinder and sphere microstructures. *J Polym Sci B Polym Phys* 35:2811–2823
- Sakamoto N, Hashimoto T (1998) Ordering dynamics of cylindrical and spherical microdomains in polystyrene-block-polyisoprene-block-polystyrene. 1. SAXS and TEM observations for the grain formation. *Macromolecules* 31:8493–8502
- Schwab M, Stühn B (1996) Thermotropic transition from a state of liquid order to a macrolattice in asymmetric diblock copolymers. *Phys Rev Lett* 76:924–927
- Sebastian JM, Graessley WW, Register RA (2002a) Steady-shear rheology of block copolymer melts and concentrated solutions: defect-mediated flow at low stresses in body-centered-cubic systems. *J Rheol* 46:863–879
- Sebastian JM, Lai C, Graessley WW, Register RA (2002b) Steady shear rheology of block copolymer melts: zero shear viscosity and shear disordering in body centered cubic systems. *Macromolecules* 35:2700–2706
- Shin G, Sakamoto N, Saijo K, Suehiro S, Hashimoto T, Ito K, Amemiya Y (2000) Time-resolved SAXS studies of a sphere forming block copolymer under large oscillatory shear deformation. *Macromolecules* 33:9002–9014
- Soenen H, Berghmans H, Winter HH, Overbergh N (1997) Ordering and structure formation in triblock copolymer solutions. Part I. Rheological observations. *Polymer* 22:5653–5660
- Tan H, Watanabe H, Matsumiya Y, Kanaya T, Takahashi Y (2003) Shear induced disruption and recovery of microphase-separated network of BSB triblock copolymer in dibutyl phthalate. *Macromolecules* 36:2886–2893
- Watanabe H, Matsumiya Y, Kanaya T, Takahashi Y (2001a) Rheology and structure of a butadiene–styrene diblock copolymer in dibutyl phthalate: role of concentration fluctuation in disruption and reformation of micellar lattice. *Macromolecules* 34:6742–6755
- Watanabe H, Kanaya T, Takahashi Y (2001b) Equilibrium elasticity of diblock copolymer micellar lattice. *Macromolecules* 34:662–665
- Winter HH, Chambon F (1986) Analysis of linear viscoelasticity of a crosslinking polymer at the gel point. *J Rheol* 30:367–382
- Winter HH, Mours M (1997) Rheology of polymers near their liquid–solid transitions. *Adv Polym Sci* 134:165–234
- Winter HH, Scott DB, Gronski W, Okamoto S, Hashimoto T (1993) Ordering by flow near the disorder–order transition of a triblock copolymer styrene–isoprene–styrene. *Macromolecules* 26:7236–7244